
Underwater Acoustic Measurements from Washington State Ferries 2006 Mukilteo Ferry Terminal Test Pile Project



Prepared for

Washington State Ferries &
Washington State Department of Transportation

March 2007

Underwater Acoustic Measurements from Washington State Ferries 2006 Mukilteo Ferry Terminal Test Pile Project

Prepared by

Alex MacGillivray



2101 – 4464 Markham Street
Victoria, British Columbia, Canada V8Z 7X8

with contributions from

Ellie Ziegler

Environmental Compliance
Washington State Ferries

and

Jim Laughlin

Asst. Air, Noise, and Energy Program Manager
Washington State Dept. of Transportation

Prepared for

**Washington State Ferries &
Washington State Department of Transportation**

Version 2
March 6, 2007

Suggested format for citation:

MacGillivray, A., Ziegler, E. and Laughlin, J., 2007. Underwater Acoustic Measurements from Washington State Ferries 2006 Mukilteo Ferry Terminal Test Pile Project. Technical report prepared by JASCO Research, Ltd for Washington State Ferries and Washington State Department of Transportation, 27 pp.

Table of Contents

Table of Contents	iv
List of Tables	iv
List of Figures	iv
1 Introduction.....	1
2 Project description	1
3 Experiment description	2
4 Methodology.....	5
4.1 Measurement apparatus	5
4.2 Data processing.....	7
4.3 Acoustic metrics.....	7
4.3.1 Impulsive noise.....	7
4.3.2 Continuous noise.....	8
5 Results.....	9
5.1 Steel pile driving measurements	9
5.2 Concrete pile driving measurements.....	10
5.3 Spectral levels	11
5.4 Propagation loss	12
5.5 Seismic interface waves.....	14
5.6 Background levels.....	15
6 Discussion.....	17
6.1 Range dependence of sound attenuation.....	17
6.2 Distance to background level.....	17
6.3 Comparison with Eagle Harbor measurements.....	18
7 Summary.....	18
8 Literature cited.....	19

List of Tables

Table 1: Summary of pile type, date and time of striking, measurement distances and mitigation used for seven piles (five steel, two concrete) measured in the current study. .	5
Table 2: Mean peak and 90% <i>rms</i> SPL attenuation versus range for the double-walled TNAP, foam-walled TNAP and bubble curtain mitigation methods. The attenuation was estimated by subtracting measured levels from unmitigated levels measured during the driving of pile T2 and R2.....	10

List of Figures

Figure 1: (a) Plan view diagram showing the pile locations at the test site with depth contours in feet. (b) Photograph of the steel piles (R1-R4 and T2) and the pile driving hammer. The hammer was suspended over pile R2 and the crane barge can be seen in the background. The froth on the water was caused by the active bubble curtain.	3
--	---

Figure 2: Photographs of attenuation methods tested during the current study: (a) Foam-walled TNAP (inset shows detail of foam); (b) double-walled TNAP; (c) bubble curtain; (d) wood pile caps..... 3

Figure 3: USGS aerial photomosaic of study site with annotations showing OBH deployment locations (A, B, C and D) and pile driving site..... 4

Figure 4: Photograph of a JASCO autonomous Ocean Bottom Hydrophone (OBH) recorder system. The OBH stands approximately 1 meter tall. 6

Figure 5: Average (a) peak and (b) 90% RMS sound pressure levels versus range for the steel piles (R1-R4 and T2) measured on 16 November 2006..... 10

Figure 6: Average (a) peak and (b) 90% RMS sound pressure levels versus range for the concrete piles (T3 and T4) measured on 5 December 2006. 11

Figure 7: Plots of mean spectral energy levels as a function of range for steel and concrete piles measured during the Test Pile project..... 12

Figure 8: Acoustic propagation loss versus range for (a) peak and (b) 90% *rms* level data fit by least-squares analysis to pile T2 data. Dashed line indicates the best fit to the data; the equation with the fit parameters is shown in the plot annotation..... 13

Figure 9: Waveform plots showing seismic interface waves (Scholte waves) generated during the driving of pile T2 at 10 meters, 50 meters and 100 meters distance. The Scholte waves are indicated by arrows on the plots. Note that the waveforms have been amplified to emphasize the interface waves. 15

Figure 10: Continuous background measurements at station “D” (1.1 km) for 16 November. Top plot shows broadband 1-minute average sound levels versus time. Bottom plot shows spectral power levels versus time. Times are given in hours from midnight on 16 November. 16

Figure 11: Histogram of 1 minute L_{eq} background levels for 7 hours at station “D” on 16 November. Percentiles ambient noise levels from the histogram are shown in the plot annotation. Note that the $N\%$ percentile noise level is defined as the L_{eq} that was exceeded during $N\%$ of the total recording time. 16

1 Introduction

This report presents measurements of underwater sound pressure levels from marine impact pile driving taken by JASCO Research Ltd during Washington State Ferries' 2006 Test Pile project. Acoustic recordings were obtained using several autonomous OBH (*Ocean Bottom Hydrophone*) recorder systems deployed at various ranges from the pile driving. The primary goals of this study were to quantify sound levels as a function of distance from impact pile driving at the Mukilteo test site and to compare the effectiveness of different noise attenuation methods. A secondary goal of this study was to measure ambient noise levels at the test site in order to estimate the distance at which the pile driving noise fell below the background level.

The Test Pile project was carried out at an abandoned fuelling pier nearby the Mukilteo Ferry terminal during November and December of 2006. Sound pressure levels were measured during the driving of five steel piles on November 16 and two concrete piles on December 5 at distances between 50 meters (55 yards) and 1100 meters (1200 yards) from the piles. Ambient noise recordings were also obtained using a high sensitivity hydrophone on November 16. Additional pile driving data were recorded at 10 meters range (11 yards) by Washington State Department of Transportation. These additional data were provided to JASCO for analysis and are also presented in this report.

2 Project description¹

Washington State Ferries (WSF) plans to relocate the Mukilteo Ferry Terminal approximately 1,400 feet east from its existing location to the Tank Farm property. The purpose of the Mukilteo Test Pile Program (project) was to test the feasibility of using hollow, pre-cast, concrete piles and/or solid concrete piles for the Mukilteo Multimodal Ferry Terminal project and future ferry terminal projects as an alternative to using steel piles. The following pile types and sizes were installed for testing:

- Five 36-inch diameter, hollow, steel piles
- Two 36-inch diameter, hollow, concrete piles
- One 24-inch diameter, octagonal, concrete pile

In addition to evaluating the constructability aspects of these piles (i.e., can they be driven at this site using conventional pile-driving equipment without damage to the pile), the project also conducted extensive in-air and under water noise measurements to determine the noise levels created by the different pile types and to test different noise attenuation methods. The following noise attenuation systems were tested:

- Bubble Curtain
- Foam-walled steel noise attenuation pile (foam-walled TNAP²)
- Double-walled steel noise attenuation pile (double-walled TNAP)

¹ This section contributed by Ellie Ziegler, Environmental Compliance, Washington State Ferries

² TNAP stands for *Temporary Noise Attenuation Pile*.

3 Experiment description

Acoustic pressure waveforms were measured during the driving of steel and concrete piles at a condemned fueling pier located nearby Washington State Ferries' Mukilteo terminal in Mukilteo, Washington. A plan view diagram showing the position of the piles at the test site is shown in Figure 1(a). The construction contractor conducted the pile driving from an anchored crane barge located next to the piles. Five steel piles (R1, R2, R3, R4 and T2) were driven on November 16 and two concrete piles (T3 and T4) were driven on December 1 ("R" and "T" indicated reaction piles and test piles, respectively). The steel piles had 36" outer diameter and 1" wall thickness (~372 lbs./ft. weight per unit length) and the concrete piles had 36" outer diameter and 4" wall thickness (~419 lbs./ft. weight per unit length). The piles were driven using a Delmag D62 diesel impact hammer suspended from a floating crane. The weight of the hammer piston was 14,600 lbs. and the total stroke of the piston varied between 5 ft. and 9 ft. during the pile driving. A photograph of the steel piles and the pile driving hammer is shown in Figure 1(b).

Noise mitigation for piles R1, R3 and R4 was achieved using a 54" diameter steel sheath fitted around the pile, referred to as a "TNAP" (*Temporary Noise Attenuation Pile*). Two different TNAP designs were evaluated during the Test Pile measurements: a foam-walled TNAP (see Figure 2(a)) and a double-walled TNAP (see Figure 2(b)). The foam-walled TNAP had a 2" layer of foam attached to the inside of the TNAP sleeve. The foam layer was covered by thin perforated steel sheets. The double-walled TNAP had a 48" diameter steel inner wall (3/8" thick) and the space between the two steel walls was air filled. Note, however, that the double-walled TNAP that was used for the November 16 tests failed due to water leaking into the air-filled cavity between the steel walls.

Noise mitigation for piles R2 and T2 was achieved using a bubble curtain (see Figure 2(c)). The bubble curtain apparatus consisted of two perforated metal rings which were connected via air hoses to an air compressor. The bubble curtain was suspended over the pile during the pile driving and, while the bubble curtain was active, the air compressor supplied the aerating rings at a rate of 400 CFM (cubic feet per minute) at 75 psi air pressure.

Wood pile caps of 12" thickness were placed over the ends of the concrete piles (T3 and T4) by the construction contractor to prevent the piles from shattering (see Figure 2(d)). Although the primary purpose of the wood caps was to protect the piles, these caps also served to reduce the impulse delivered to the piles by the impact hammer and were expected to reduce noise levels from the driving of the concrete piles. Previous measurements by WSDOT (J. Laughlin, pers. comm.) have shown that wood pile caps are effective for mitigating underwater noise levels generated by marine pile driving.

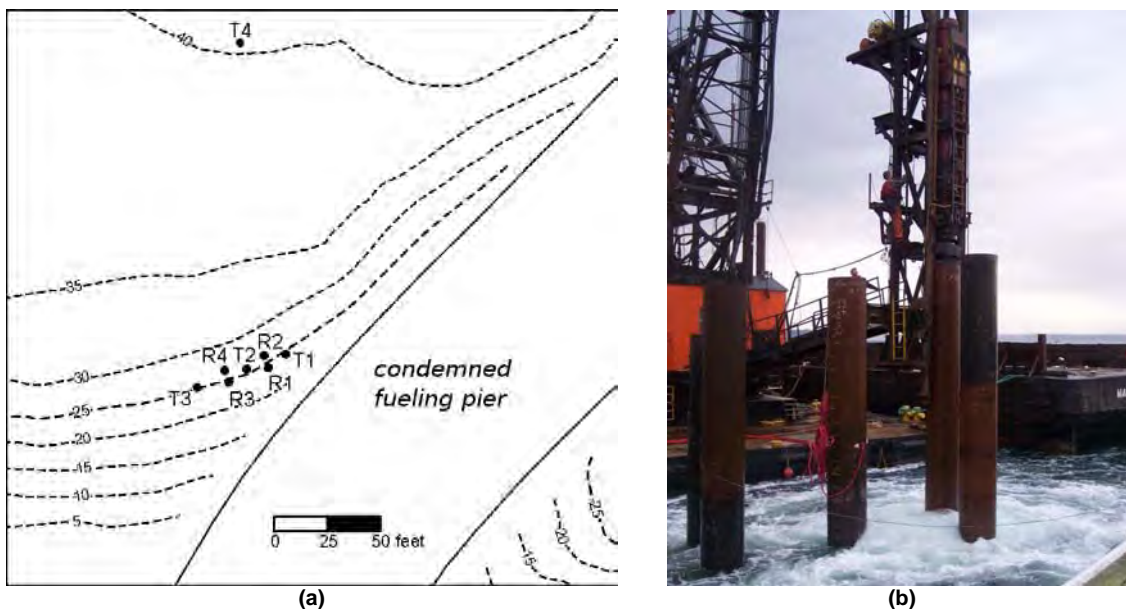


Figure 1: (a) Plan view diagram showing the pile locations at the test site with depth contours in feet. (b) Photograph of the steel piles (R1-R4 and T2) and the pile driving hammer. The hammer was suspended over pile R2 and the crane barge can be seen in the background. The froth on the water was caused by the active bubble curtain.

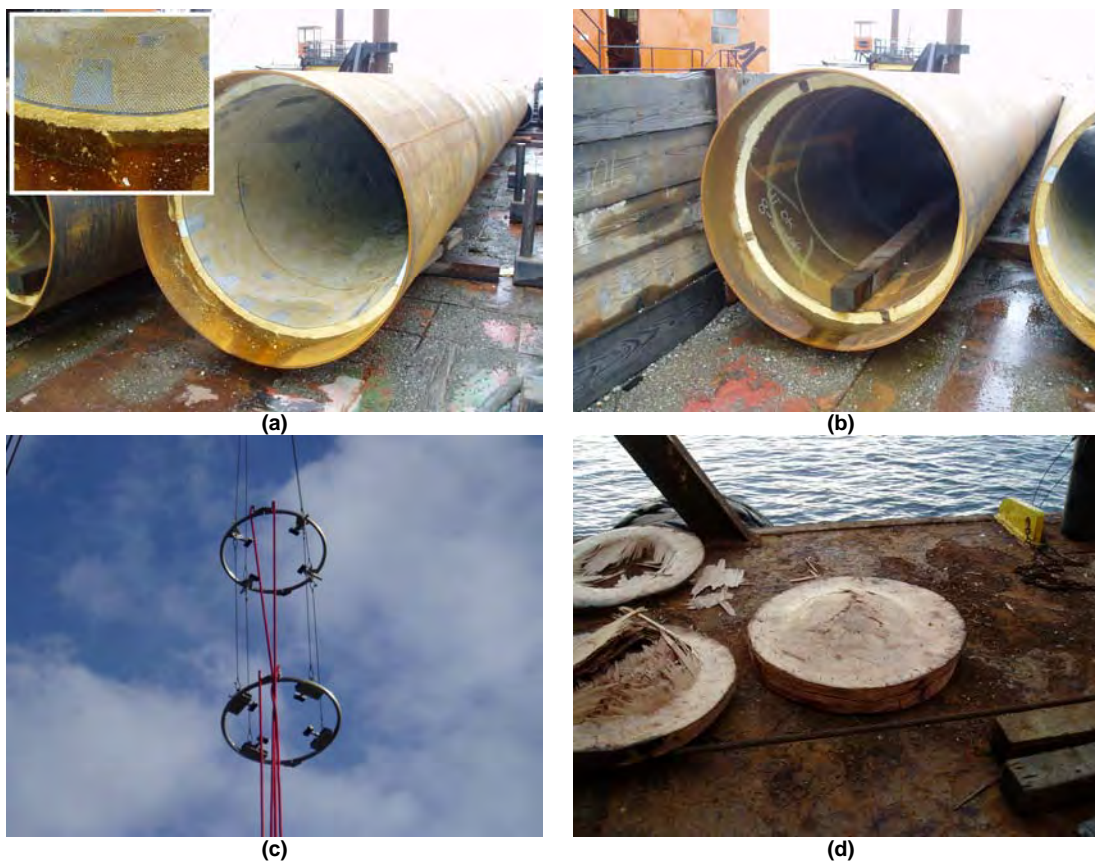


Figure 2: Photographs of attenuation methods tested during the current study: (a) Foam-walled TNAP (inset shows detail of foam); (b) double-walled TNAP; (c) bubble curtain; (d) wood pile caps.

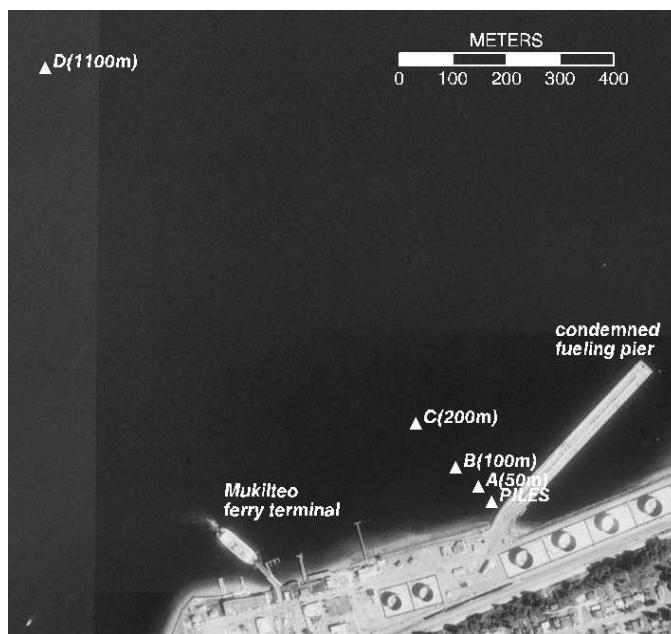


Figure 3: USGS aerial photomosaic of study site with annotations showing OBH deployment locations (A, B, C and D) and pile driving site.

JASCO obtained acoustic measurements using three autonomous Ocean Bottom Hydrophone (OBH) recorders deployed at a total of four different recording stations, designated “A” through “D” respectively. The locations and distances of the four recording stations from the pile driving are shown in Figure 3. Distances from the piles to recording stations A–C were measured using a laser range finder; the distance to station D was computed from GPS measurements. The UTM locations of all the recording stations were measured using a hand-held GPS unit. Ambient noise recordings were obtained at stations C and D using an additional high sensitivity hydrophone mounted on the far OBH system.

The OBH’s were initially deployed on November 14–15 at stations A, B and C but only sporadic pile driving was recorded during this period due to problems with the pile driving hammer. The OBH’s were re-deployed on November 16 at stations A, B and D and acoustic data were obtained during the successful driving of all the steel piles (R1, R2, R3, R4 and T2). On December 5, during the driving of two of the concrete piles (T3 and T4), a single OBH was deployed at station C and a surface-based acoustic recording system was deployed at station A. The surface-based acoustic recording system consisted of a tethered hydrophone which was lowered over the side of the crane barge at 50 meters range from the piles.

Table 1: Summary of pile type, date and time of striking, measurement distances and mitigation used for seven piles (five steel, two concrete) measured in the current study.

Pile	Type	Date	Time	Measurement ranges (m)	Bubble curtain	DW TNAP	Foam TNAP	Wood cap
R4	Steel	16-Nov-06	09:00:00	10, 50, 100, 1100		x		
R3	Steel	16-Nov-06	09:45:00	10, 50, 100, 1100			x	
R2	Steel	16-Nov-06	11:00:00	10, 50, 100, 1100	x			
R1	Steel	16-Nov-06	13:00:00	10, 50, 100, 1100			x	
T2	Steel	16-Nov-06	14:30:00	10, 50, 100, 1100	x			
T3	Concrete	05-Dec-06	09:30:00	50, 200				x
T4	Concrete	05-Dec-06	13:30:00	50, 200				x

Table 1 presents a summary of the date, time, recording locations and mitigation methods for each of the piles measured in the current study. Additional acoustic pile driving data for November 16 were recorded at 10 meters distance by Jim Laughlin of Washington State Department of Transportation. These data were provided to JASCO for inclusion in this report. Note that the 10 meter data were recorded mid-water-column, rather than at the seabed as with the OBH measurements.

4 Methodology

4.1 Measurement apparatus

Three autonomous JASCO Ocean Bottom Hydrophone (OBH) recorders were used for obtaining acoustic measurements for the current study; a photograph of one of the OBH systems is shown in Figure 4. The OBH systems consisted of the following components:

1. An aluminum pressure case containing a digital audio recorder and batteries
2. Either one or two calibrated reference hydrophones
3. An acoustic release system
4. Four fiberglass floats

The OBH systems used two different kinds of calibrated reference hydrophones for the acoustic recordings:

1. A Reson TC4043, with nominal sensitivity -201 dB re V/ μ Pa.
2. A Reson TC4032, with nominal sensitivity -170 dB re V/ μ Pa.

These two hydrophones, with 31 dB difference in sensitivity, provided a wide dynamic range that permitted accurate capture of both very high (i.e., pile driving) and very low (i.e., ambient noise) sound levels. The hydrophone signals were digitized using a Sound Devices model 722 hard-disk recorder housed within the OBH pressure case. The hydrophone signals were digitized at a sampling rate of 32 kHz with 24-bit precision onto a 40 GB internal hard-disk capable of storing up to 60 hours of audio data.



Figure 4: Photograph of a JASCO autonomous Ocean Bottom Hydrophone (OBH) recorder system. The OBH stands approximately 1 meter tall.

All hydrophones used in the OBH systems were calibrated according to NIST traceable standards. Additionally, the voltage and frequency response of the OBH recorders was fully calibrated in the lab prior to carrying out the acoustic measurements. The OBH recorders were calibrated by inserting a reference signal, with known amplitude and frequency, into the calibration lines of the OBH hydrophones. The voltage calibration of the systems was obtained from the level of the reference signal on the digital recorders. The voltage insertion test combined with the pressure calibration of the hydrophones yielded an end-to-end calibration of the combined acoustic and electrical response of the OBH systems.

The OBH's were deployed over the side of a small boat and moored on the seabed using sacrificial concrete anchor weights attached to the OBH via an acoustic release system. Since the OBH systems were resting on the seabed, the OBH measurements from this study were obtained 1 meter above the bottom depth at each measurement site. After the measurements were completed, the OBH systems were detached from their anchors using the acoustic releases and retrieved using a small boat.

For the December 5 measurements, when only a single OBH was available, additional acoustic measurements were obtained using a surface-based acoustic recording system. The surface-based system consisted of a single Reson TC4043 hydrophone (-201 dB re V/ μ Pa) which was suspended 1 meter from the bottom using a hydrophone cable tethered to the surface. The hydrophone was deployed off the side of the crane barge and the hydrophone signal was fed to a manually operated Marantz PMD690 acoustic recorder. The acoustic signal from the surface-based system was digitized at 48 kHz with 16-bits precision onto IBM Microdrive media. The surface-based recorder was calibrated according to the same procedures as the OBH systems.

4.2 Data processing

Custom software, written in the IDL data analysis language, was used to analyze acoustic waveform data from the pile driving. The processing steps were as follows:

1. Pile driving impulses in the acoustic recordings were identified using a combination of manual picks and automated detection.
2. Waveform data were converted to units of μPa using the calibrated acoustic response of each OBH system.
3. Waveforms were filtered above 15 Hz to remove low-frequency vessel traffic noise and to prevent smearing of the 90% *rms* level from late-arriving Scholte-waves (see Section 5.5).
4. Each pile driving impulse was analyzed to determine peak-to-peak level, peak level, 90% *rms* level and sound exposure level (see next section).
5. Each pile driving impulse was transformed to the frequency domain, via the Fast Fourier Transform, to obtain 1-Hz spectral power levels.

4.3 Acoustic metrics

4.3.1 Impulsive noise

For the current study, the following standard metrics have been used for reporting received sound pressure levels from impulsive pile-driving noise (see ANSI S1.1-1994). Note that, in the following definitions, the measured acoustic pressure of the impulse event is $p(t)$, the total length of the pulse is T and $0 < t < T$:

1. **Peak-to-peak Sound Pressure Level**, measured in dB re μPa , is the difference between the maximum and minimum overpressure for an impulsive event:

$$L_{pk-pk} = 20 \log_{10} (\max(p(t)) - \min(p(t))) \quad (1)$$

2. **Peak Sound Pressure Level**, measured in dB re μPa , is the maximum absolute values of the overpressure for an impulsive event:

$$L_{pk} = 20 \log_{10} (\max(|p(t)|)) \quad (2)$$

3. **90% RMS Sound Pressure Level**, measured in dB re μPa . This metric is defined as the root-mean-square sound pressure level over a period T_{90} that contains 90% of the pulse energy:

$$L_{P90} = 20 \log_{10} \left(\sqrt{\frac{1}{T_{90}} \int_{T_{90}} p(t)^2 dt} \right) \quad (3)$$

4. **Sound Exposure Level**, measured in dB re $\mu\text{Pa}^2 \cdot \text{s}$. For a single pulse, the sound exposure is defined as the integral of the squared sound pressure over the duration of the pulse event (see section 3.54 of ANSI S1.1-1994):

$$L_E = 10 \log_{10} \left(\int_T p(t)^2 dt \right) \quad (4)$$

For multiple impulsive events, the total sound exposure level is computed as the

decibel sum of the sound exposure of the individual events.

$$L_E^{(tot)} = 10 \log_{10} \sum 10^{L_E^i / 10} \quad (5)$$

In addition, spectral energy levels for pile driving impulses have been computed from the Fourier transform of the pile driving waveforms:

$$E(f) = 10 \log \left(\left| \int_T p(t) \exp(-2\pi f t) dt \right|^2 \right) \quad (6)$$

where f is the sound frequency in units of Hz and $E(f)$ is the spectral energy level at frequency f . Spectral energy levels for pile driving impulses are reported in units of dB re $\mu\text{Pa}^2 \cdot \text{s}/\text{Hz}$. Note that no frequency weighting (*e.g.*, A-weighting or C-weighting) has been applied to the acoustic measurements presented in this report.

4.3.2 Continuous noise

Broadband ambient (background) noise levels from this study have been reported in terms of the 1 minute average continuous sound level (1 minute L_{eq}):

$${}^{(1\text{min})} L_{eq} = 10 \log \left(\frac{1}{T} \int_T p(t)^2 dt \right) \quad (7)$$

where $p(t)$ is the acoustic overpressure, $T = 60$ seconds and $0 < t < T$. Thus, the 1-minute L_{eq} is the *rms* sound pressure level over a 1-minute period. Average spectral power levels for ambient noise have been computed from the Fourier transform of pressure waveforms in 1 minute time intervals:

$${}^{(1\text{min})} P(f) = 10 \log \left(\frac{1}{T} \left| \int_T p(t) \exp(-2\pi f t) dt \right|^2 \right) \quad (8)$$

where f is the sound frequency in units of Hz, $P(f)$ is the spectral power level at frequency f and $T = 60$ s. Note that spectral power levels are reported in units of dB re $\mu\text{Pa}^2/\text{Hz}$ and that no frequency weighting (*e.g.*, A-weighting or C-weighting) has been applied to the acoustic measurements presented in this report. All sound levels quoted in this report are given in decibels relative to the standard underwater acoustic reference pressure of 1 μPa .

5 Results

5.1 Steel pile driving measurements

Figure 5 shows plots of peak and 90% *rms* sound pressure level (SPL) versus range for the November 16 pile driving measurements. Sound level versus range data are presented for all five steel piles (R1–R4 and T2). For piles R2 and T2, separate SPL's were computed for measurements taken with and without bubble curtain mitigation. Each data point represents the mean SPL averaged over multiple blows from the pile driving hammer. Maximum measured peak SPL's were 1.7–4.7 dB greater than mean levels and maximum measured 90% *rms* SPL's were 1.1–4.1 dB greater than mean levels (see Appendix A). Variations in measured sound levels between pile driving strikes were observed for all the piles; these variations were presumably caused by variations in the stroke height of the pile driving hammer.

Measurements of pile T2 and R2 taken with the bubble curtain inactive provide a useful “unmitigated” benchmark level that can be used to estimate the effectiveness of the different mitigation methods tested at the Mukilteo site. Table 2 shows the estimated attenuation versus range for the foam-walled TNAP, bubble curtain and double-walled TNAP; these attenuation factors were computed by subtracting measured pile driving sound levels from the unmitigated T2 and R2 levels for all four measurement ranges. The data for piles R1, R3 and T2 show that the foam-walled TNAP and bubble curtain were both equally effective at reducing sound levels from the pile driving; sound levels measured at 10 meters range were reduced by approximately 25 dB by both the foam-walled TNAP and the bubble curtain. However, the data also show that the effectiveness of these mitigation methods was range-dependent and that the sound attenuation diminished with range from the pile.

The double-walled TNAP that was used for the November 16 tests failed due to a leak which caused the air-filled cavity between the walls to flood with water. The failed TNAP was not found to be effective at reducing sound levels from the pile driving; the attenuation provided by the double-walled TNAP was less than 10 dB at all ranges. However, subsequent measurements taken during re-strike tests on 19 February 2007 showed that the repaired double-walled TNAP design was effective at reducing peak levels from the pile driving by 12-17 dB.

In addition to the peak and 90% *rms* levels presented in this section, peak-to-peak and sound exposure levels were also computed from the acoustic waveform data collected during the test pile study. These additional data are presented in Appendix A, which lists tables of mean and maximum sound levels versus range in terms of all four impulsive acoustic metrics discussed in Section 4.3.1.

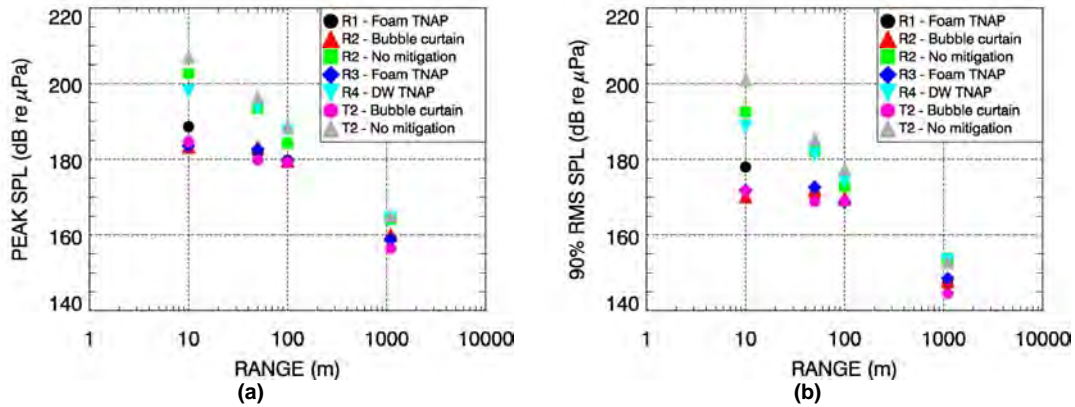


Figure 5: Average (a) peak and (b) 90% RMS sound pressure levels versus range for the steel piles (R1-R4 and T2) measured on 16 November 2006.

Table 2: Mean peak and 90% rms SPL attenuation versus range for the double-walled TNAP, foam-walled TNAP and bubble curtain mitigation methods. The attenuation was estimated by subtracting measured levels from unmitigated levels measured during the driving of pile T2 and R2.

Range (m)	Mean peak attenuation (dB)			Mean 90% rms attenuation (dB)		
	Bubble curtain	Foam TNAP	DW TNAP ^a	Bubble curtain	Foam TNAP	DW TNAP ^a
10	20.8	21.4	6.8	25.8	25.7	8.2
50	13.4	12.0	1.3	13.4	11.5	2.4
100	7.0	6.8	-1.1	5.9	6.1	0.8
1100	6.2	5.0	0.1	7.1	5.1	0.1

a) Note that the double-walled TNAP failed due to a leak in the TNAP wall during the November 16 measurements.

5.2 Concrete pile driving measurements

Figure 6 shows peak and 90% rms sound pressure levels for the driving of the concrete piles measured on December 5. Each data point represents the mean SPL averaged over multiple blows from the pile driving hammer. Maximum measured peak SPL's were 1.9–2.1 dB greater than mean levels and maximum measured 90% rms SPL's were 2.5–2.6 dB greater than mean levels (see Appendix A). Note that only two recording systems, deployed at 50 meters and 200 meters range, were used for the concrete pile measurements since the long-range transmission loss at the Mukilteo site was sufficiently well constrained by the steel pile measurements on November 16. Additional data at 10 meters range were not available for these piles. Comparison of the concrete pile driving data with the steel pile driving data at 50 meters range showed that, on average, peak levels for the concrete pile driving were 5.3 dB less than for the unmitigated steel piles and 90% rms levels were 10.0 dB less than for the unmitigated steel piles. However, concrete pile driving sound levels at 50 meters were greater than the mitigated steel pile driving levels. Additional SPL data are presented in Appendix A, which lists tables of mean and maximum sound levels versus range in terms of all four impulsive acoustic metrics discussed in Section 4.3.1.

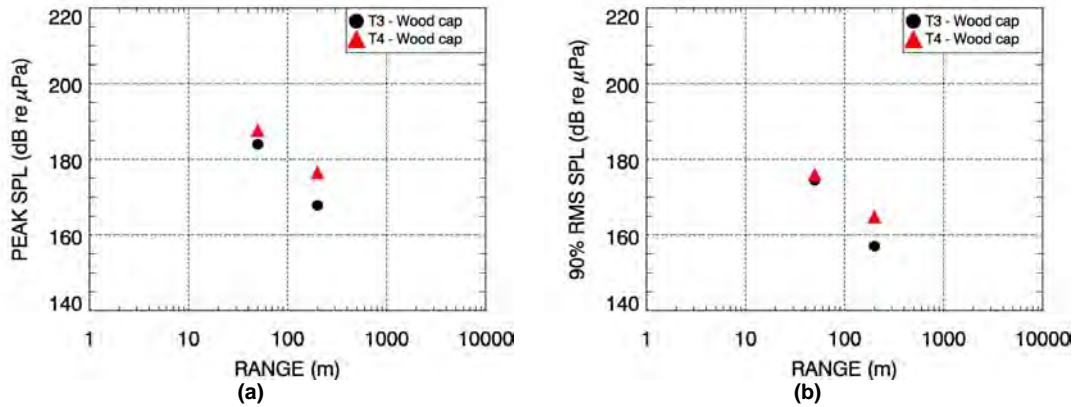


Figure 6: Average (a) peak and (b) 90% RMS sound pressure levels versus range for the concrete piles (T3 and T4) measured on 5 December 2006.

5.3 Spectral levels

Figure 7 shows plots of spectral energy levels, in 1 Hz frequency bins, as a function of range for both the steel pile and concrete pile measurements. The spectra presented in the plots are mean levels averaged over multiple impulses from the pile driving hammer. These plots show the frequency distribution of acoustic energy in the measured pile driving waveforms. Examining the spectra for piles R2 and T2 shows that most of the sound energy from the unmitigated pile driving was concentrated at frequencies below 1 kHz. Comparison of the unmitigated spectral levels to the data for the foam-walled TNAP's and bubble curtain (plots (a), (b), (d) and (e)) indicates that the mitigation was also most effective at frequencies below 1 kHz.

The most interesting feature of Figure 7 is that, while the bubble curtain was active, spectral levels below 1 kHz were approximately constant between 10 meters and 100 meters range (i.e., in plots (b) and (e) for piles R2 and T2). A similar but less exaggerated effect was observed for the foam-walled TNAP's (i.e., in plots (a) and (d) for piles R1 and R3). In contrast, spectral levels with the bubble curtain off (plots (c) and (f)) showed approximately 20 dB propagation loss between 10 meters and 100 meters range below 1 kHz. The exact physical cause of this “flattening” of the acoustic propagation loss below 1 kHz is uncertain; however, some possible explanations are discussed in Section 6.

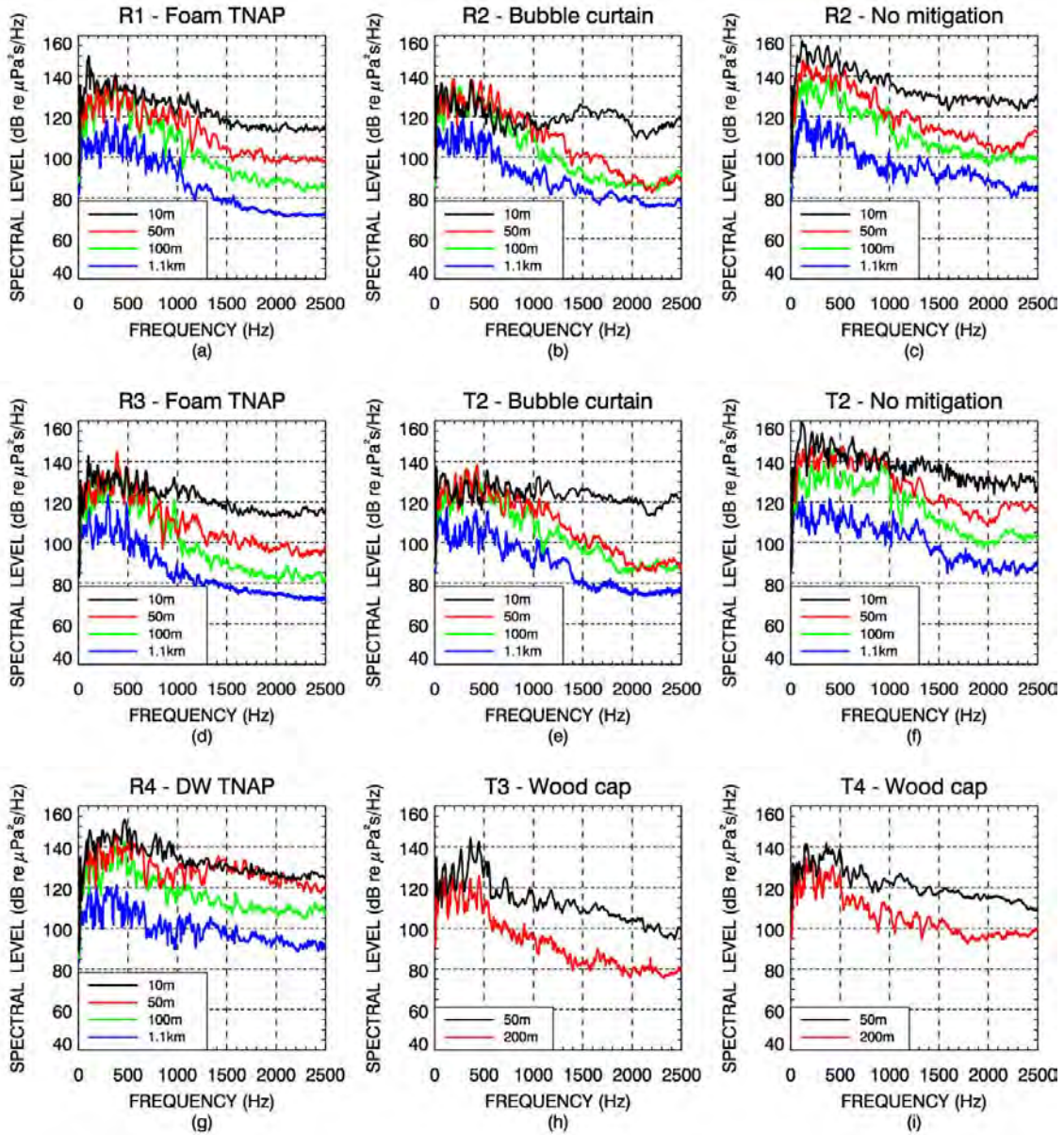


Figure 7: Plots of mean spectral energy levels as a function of range for steel and concrete piles measured during the Test Pile project.

5.4 Propagation loss

In order to estimate the acoustic propagation loss of the pile driving with range from the source, a linear transmission loss curve of the following form was fit to the peak and 90% *rms* pile driving data using the method of least squares:

$$L_p(r) = SL - A \log_{10}(r) \tag{9}$$

where $SL = L_p(r = 1)$ is the approximate source level (i.e., back-propagated to 1 meter range) and A is the geometric spreading loss parameter. Figure 8 shows the best-fit transmission loss curve for the unmitigated (i.e., with the bubble curtain off) peak and

90% *rms* sound level data for pile T2 and R2. Figure 8 shows that the acoustic propagation loss at the Mukilteo site was approximately equivalent to spherical spreading (i.e., $20 \log_{10}(r)$ transmission loss) for both peak and 90% *rms* levels. Figure 8 also shows that the estimated peak and 90% *rms* source levels of the unmitigated pile driving were approximately 226.6 dB re $\mu\text{Pa m}$ and 218.8 dB re $\mu\text{Pa m}$ respectively (i.e., the far-field levels back-propagated to 1 meter distance).

The data in Table 2 show that pile driving sound levels for the bubble curtain and foam-walled TNAP did not fall along a linear transmission loss curve (i.e., of the form given by Equation 9) because the attenuation provided by these mitigation methods was range-dependent. However, mitigated sound levels may be estimated from the propagation loss equations shown in Figure 8 by subtracting the range-dependent attenuation factors given in Table 2 from unmitigated sound levels computed using the least-squares derived laws. For example, to estimate the *rms* level at 50 meters range from the driving of a steel pile with foam TNAP mitigation, we use the following calculation:

$$L_p = 218.8 - 21.5 \log_{10}(50) - 11.5 = 170.7 \text{ dB re } \mu\text{Pa}$$

For estimating sound levels at ranges greater than 1 km, it is reasonable to use the 1 km attenuation values because the difference in attenuation between 100 m and 1 km range was only 1-2 dB. Thus, one can estimate long-range sound propagation from the mitigated pile driving by subtracting the 1 km attenuation values given in Table 2 from the transmission loss curves for the unmitigated pile driving (see Section 6.2).

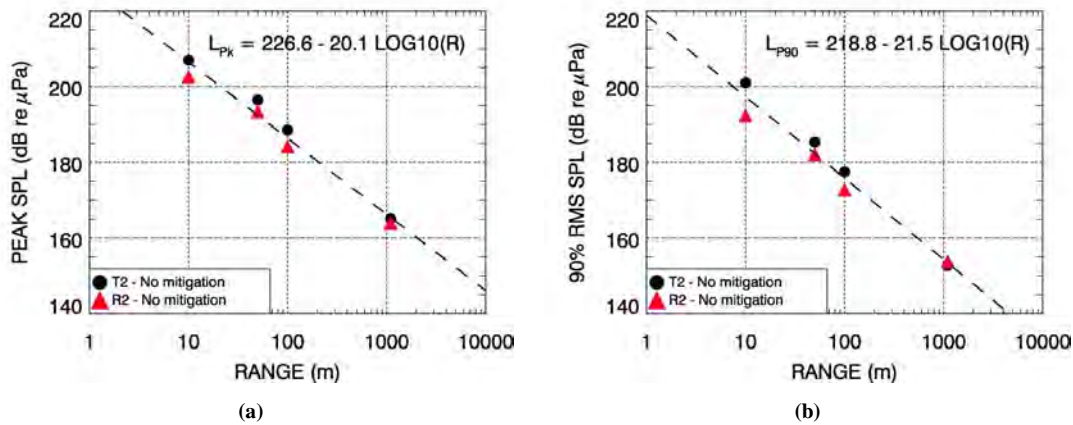


Figure 8: Acoustic propagation loss versus range for (a) peak and (b) 90% *rms* level data fit by least-squares analysis to pile T2 data. Dashed line indicates the best fit to the data; the equation with the fit parameters is shown in the plot annotation.

The wood cap mitigation used for the concrete piles was not expected to exhibit the same kind of range dependence as the bubble curtain and TNAP mitigation used for the steel piles. This is because the wood caps only affected the impulse delivered to the piles by the pile driving hammer and did not actually influence the underwater propagation environment like the TNAP or bubble curtain mitigation. Thus peak and 90% *rms* levels from the concrete pile driving may be estimated by subtracting 5 dB and 10 dB respectively from the propagation loss equation derived for the steel pile data (c.f., Section 5.2).

One should take care to consider differences in the acoustic environment when extrapolating propagation loss estimates from the Mukilteo test site to other locations. The water depth at the pile driving site was quite shallow (7-12 meters) and the bathymetry was characterized by a steeply sloping bottom that dropped away rapidly in the offshore direction at a rate of approximately 25 meters depth per 100 meters distance from shore (~14 degrees slope). As with all empirically derived transmission loss laws, the spherical spreading law derived for the Mukilteo test site should only be extrapolated to similar acoustic propagation environments.

5.5 Seismic interface waves

Another interesting feature of the pile driving data recorded at the Mukilteo test site was the presence of seismic interface waves, called “Scholte waves”, in the acoustic waveform data. Figure 9 shows an example of Scholte waves from the pile T2 recordings; note that the peaks in Figure 9 are clipped because the waveforms were amplified in order to emphasize the interface waves. The zero-time in Figure 9 is referenced to the travel time at 0 meters distance, assuming a speed of sound in water of 1.5 km/s. The Scholte waves could be distinguished from the water-borne acoustic waves by their much slower travel speed (150 m/s) and lower frequency (8 Hz-15 Hz). These seismic interface waves were presumably generated at the seabed as the piles were driven into the substrate by the pile driving hammer. Scholte waves are “inhomogeneous” waves that propagate at the boundary between a fluid medium and a solid medium — in this case at the water-seabed interface (see e.g., Jensen et al., 1994, pp. 491-492).

Scholte waves were observed in all the pile driving data, except for the recordings at station D (1100 meters range). The Scholte waves were generally much lower in amplitude than the acoustic waves by a factor of 10-30 dB. However, for processing the acoustic data it was necessary to remove the Scholte waves by applying a 15 Hz high-pass filter to the recordings. This was required because the slower Scholte waves tended to “smear out” the water-borne impulses resulting in artificially low 90% *rms* levels³. This smearing was due to the slower travel speed and long decay of the Scholte phase, which is clearly illustrated in Figure 9. Thus, high-pass filtering the data yielded more conservative measurements of the 90% *rms* SPL’s for the impulses

³ The value of the 90% *rms* level is known to be very sensitive to the integration time, T_{90} . This issue with the 90% *rms* level is well known and is discussed in greater detail the article by P.T. Madsen (2005).

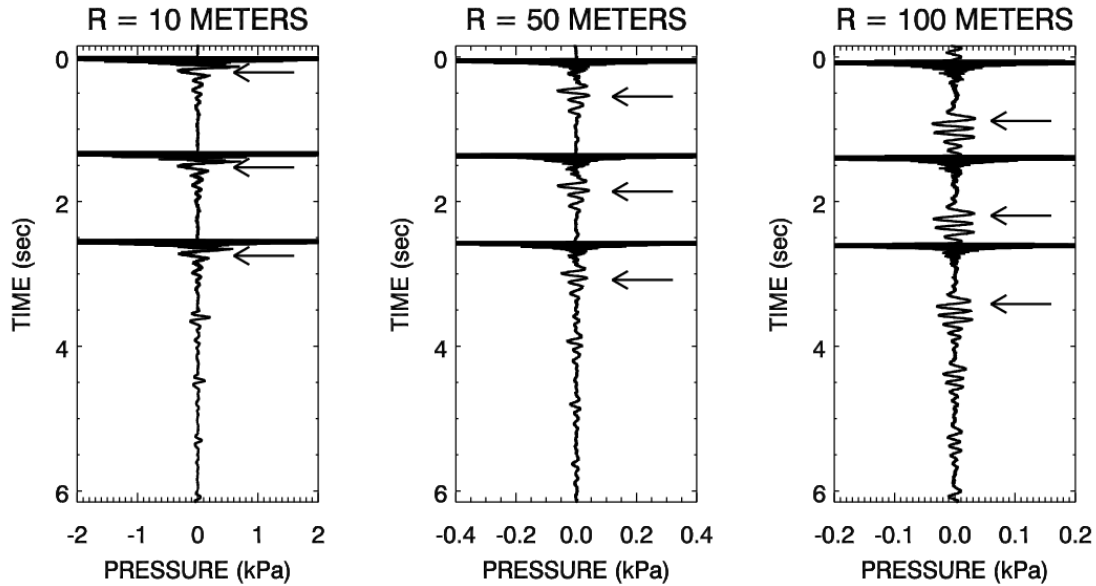


Figure 9: Waveform plots showing seismic interface waves (Scholte waves) generated during the driving of pile T2 at 10 meters, 50 meters and 100 meters distance. The Scholte waves are indicated by arrows on the plots. Note that the waveforms have been amplified to emphasize the interface waves.

5.6 Background levels

Figure 10 shows background levels measured at OBH station D on November 16 for a 7 hour period starting at 08:00 h and ending at 15:00 h. The top plot shows broadband 1 minute average sound levels (i.e., 1 minute L_{eq} 's) and the bottom plot shows spectral power levels versus time. The background noise level data were recorded using a higher sensitivity hydrophone (-170 dB re V/ μ Pa) mounted on the far OBH system.

Most of the background noise in Figure 10 corresponds to ferry traffic and other miscellaneous vessel traffic operating in the vicinity of the Mukilteo test site. The spectral plot shows that most of the vessel traffic noise was concentrated in the frequency range 20 Hz – 1 kHz, with maximum levels observed below 100 Hz. At this range (1100 meters) the increase in the 1 minute L_{eq} from intermittent pile driving was nearly the same as the increase from passing vessel traffic. Pile driving may be distinguished from vessel traffic in the spectrogram plots by the presence of spectral peaks in the 200–500 Hz frequency range.

Figure 11 shows a histogram plot of the 1 minute L_{eq} 's measured at recording station D. This histogram is divided into 1 dB intervals and shows the time distribution of background levels measured at station D on November 16. Figure 11 also shows percentile noise level statistics computed from the ambient noise histograms, where the $N\%$ noise level is the L_{eq} that was exceeded during $N\%$ of the total recording time. Daytime ambient levels at site D varied between 134.9 dB (90% level) and 119.8 dB (10% level). The 50th percentile level of the ambient noise at station D was 123.7 dB; this is a reasonable estimate of the average background ambient noise level at this location during the daytime when pile driving is most likely to occur.

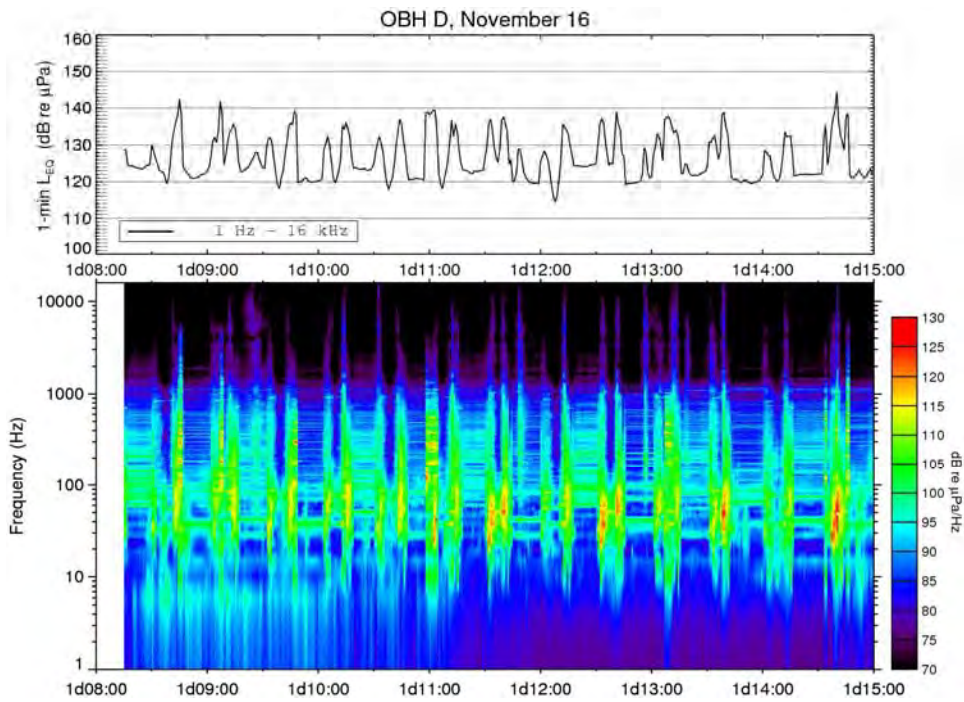


Figure 10: Continuous background measurements at station “D” (1.1 km) for 16 November 2006. Top plot shows broadband 1-minute average sound levels versus time. Bottom plot shows spectral power levels versus time. Times are given in hours from midnight.

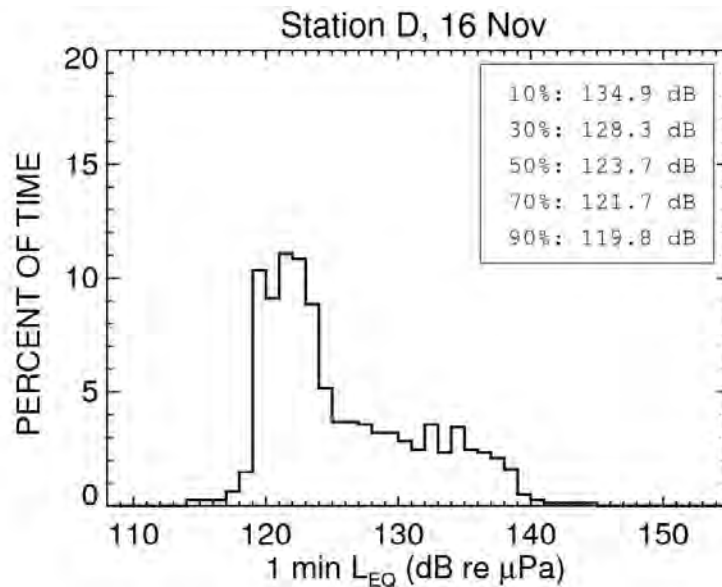


Figure 11: Histogram of 1 minute L_{eq} background levels for 7 hours at station “D” on 16 November 2006. Percentiles ambient noise levels from the histogram are shown in the plot annotation. Note that the $N\%$ noise level is defined as the L_{eq} that was exceeded during $N\%$ of the total recording time.

6 Discussion

6.1 Range dependence of sound attenuation

The foam-walled TNAP and bubble curtain mitigation systems both proved very effective at reducing sound levels from marine pile driving at short range; the sound attenuation from both systems was approximately 20 dB at 10 meters distance from the steel piles. However, the sound level attenuation of these systems was also observed to fall off with range from the pile driving; the *rms* level attenuation at 1100 meters was only about 6 dB (see Table 2). Spectral analysis showed that the range-dependence of the sound attenuation was most prominent at frequencies below 1 kHz; mitigated sound levels at these frequencies were nearly constant between 10 meters and 100 meters range (see Figure 7). One possible explanation for this effect is that acoustic impulses measured at longer ranges travelled partially through the sub-bottom, rather than directly through the water, and were thus less influenced by the bubble curtain and foam TNAP mitigation. It is also possible that the sloping bathymetry at the Mukilteo test site may have contributed to this effect. However, the precise physical cause for the range-dependence of the sound attenuation is uncertain.

6.2 Distance to background level

Ambient measurements from this study may be used to estimate the range at which the pile driving noise would fall below the background level at the Mukilteo test site. Average daytime background levels measured in the channel (i.e., at station D on November 16) were 123.7 dB (50th percentile noise level from Figure 11(b)). The range at which the *rms* level from the pile driving equals the *rms* background level is given by the following equation:

$$R = 10^{\left(\frac{SL - NL}{A}\right)} \quad (10)$$

where R is the detection limit, SL and A are the source level and spreading loss term from Equation 9, and NL is the background ambient noise level. Using this relationship and the fit parameters from Figure 8(b), *rms* levels from the unmitigated steel piles would fall below the daytime background level in the channel at ranges beyond 26.5 km. If we assume that long-range mitigated levels are 6 dB less than unmitigated levels (average attenuation at 1.1 km distance from Table 2) then the mitigated steel pile driving levels would fall below the daytime background levels beyond 13.9 km. Likewise, if we assume *rms* levels from the concrete pile driving are 10 dB less than the steel pile driving levels then the range to the background level for the concrete piles is 9.1 km.

When considering the range-to-background calculations, it is important to keep in mind that small dB uncertainties in the source level, noise level, or spreading loss may result in large uncertainties in the range predictions. For example, measured levels from the pile driving were observed to vary by about 3 dB between strikes from the impact hammer, depending on the stroke of the hammer. Assuming a propagation loss coefficient of 21.5, this would result in a 38% variation in the range to background. Thus, given a range to

background of 13.9 km for the mitigated steel piles, the expected variation in the range to background is ± 2.7 km. Note that this is neglecting additional uncertainties due to variations in the background level. The reason for the large uncertainty in the range estimate is the geometric decay of the sound levels with range from the source: in general, sound decays rapidly with range close to the source and very gradually with range far from the source.

6.3 Comparison with Eagle Harbor measurements

Unmitigated steel pile driving sound levels measured during the Mukilteo Test Pile study were slightly higher than sound levels measured by JASCO in 2005 during the Eagle Harbor pile driving study (MacGillivray and Racca, 2005). Average unmitigated peak and *rms* sound levels measured at 10 meters range for the Eagle Harbor study were approximately 203 dB re μPa and 193 dB re μPa , respectively, which were 5 dB and 8 dB less, respectively, than sound levels measured during the current study for the unmitigated T2 pile. The pile driving hammer used at Eagle Harbor was the same but the 30" steel piles driven at Eagle Harbor were slightly smaller diameter than the 36" diameter steel piles driven at Mukilteo. No concrete piles were driven during the Eagle Harbor study.

The sleeve-style bubble curtain employed at Eagle Harbor in 2005 was less effective than the foam TNAP and bubble curtain mitigation used for the current study; the former achieved only a 10 dB reduction in the *rms* level at 10 meters range whereas the latter systems achieved a 25 dB reduction in the *rms* level at 10 meters range. Sound level measurements at Eagle Harbor were taken at ranges less than 20 meters from the piles so it is unknown whether the attenuation from the bubble curtain was range-dependent as was observed in the current study.

7 Summary

For the current study, underwater sound levels were measured at distances of 10–1100 meters from the impact driving of five 36" diameter steel piles and two 36" diameter concrete piles. In addition, three different noise attenuation systems were tested during the pile driving measurements (foam-walled TNAP, double-walled TNAP and bubble curtain). The foam-walled TNAP and bubble curtain systems were both very effective at reducing sound levels from the pile driving, both achieving an average reduction of 25 dB in the *rms* level at 10 meters range. The double-walled TNAP was not effective at reducing noise levels from the pile driving due to a leak in the TNAP wall (although subsequent re-testing of the double-walled TNAP showed that it was effective at reducing noise levels from the pile driving by 12–19 dB).

The effective attenuation of both the foam TNAP and bubble curtain mitigation were observed to decrease with range from the pile driving. Although the *rms* level attenuation from these systems at 10 meters range was 25 dB, their effective attenuation at 1100 meters ranges was only 6 dB. The range-dependence of the attenuation resulted in a pronounced flattening of the acoustic propagation loss at ranges less than 100 m from

the pile driving. Spectral analysis of the pile driving waveforms showed that the sound attenuation of the foam TNAP and bubble curtain was most effective at frequencies below 1 kHz. The flattening of the propagation loss at short range meant that sound levels at frequencies below 1 kHz were nearly constant at ranges less than 100 meters.

For the unmitigated pile driving, sound level versus range measurements indicated that transmission loss at the Mukilteo test site was approximately equivalent to spherical (i.e., $20 \log_{10} r$) spreading. The empirically measured propagation loss was used to derive source levels for the unmitigated steel pile driving: peak and *rms* source levels were estimated to be 226.6 dB re $\mu\text{Pa m}$ and 218.8 dB re $\mu\text{Pa m}$, respectively. Peak and *rms* sound levels for the concrete pile driving were estimated to be 5 dB and 10 dB less, respectively, than levels from the unmitigated steel pile driving.

In addition to the pile driving data, ambient noise recordings were obtained in the channel on 16 November 2006 at 1.1 km distance from the Mukilteo test site. Analysis of the recordings showed that daytime ambient noise levels at the recording site were dominated by noise from nearby vessel traffic. A statistical analysis showed that daytime ambient levels varied by over 15 dB at station D (10% and 90% ambient noise levels were 119.8 and 134.9 dB, respectively). Average daytime noise levels in the channel were measured to be 123.7 dB re μPa (50th percentile L_{eq}). Based on the measured ambient noise levels, and the observed decay of pile driving levels with range, the range to background for the unmitigated steel piles, mitigated steel piles and concrete piles were estimated to be 26.5 km, 13.9 km and 9.1 km, respectively. Note, however, that the uncertainty in these range estimates is large due to the observed variations in both the loudness of the pile driving and the measured background levels at the test site.

Finally, seismic interface waves (Scholte waves) were clearly observed in the acoustic pile driving waveforms. These waves were present at very low frequencies (8 Hz to 15 Hz) and travelled much slower than the water-borne acoustic waves (~150 m/s). These Scholte waves were most likely generated at the seabed as the piles were driven into the substrate. The Scholte waves were only detected at ranges less than 200 meters from the pile driving.

8 Literature cited

ANSI S1.1 *American National Standard Acoustical Terminology*. 1994.

Jensen, F.B., Kuperman, W.A., Porter, M.B. and Schmidt, H., *Computational Ocean Acoustics*. AIP Press, Woodbury, NY. 1994.

MacGillivray, A.O. and Racca, R., "Sound pressure and particle velocity measurements from marine pile driving at Eagle Harbor maintenance facility, Bainbridge Island, WA." Technical report prepared for Washington State Department of Transportation by JASCO Research Ltd. November 2005.

Madsen, P.T., "Marine mammals and noise: problems with root mean square sound pressure level for transients." *Journal of the Acoustical Society of America*. v. 117, pp. 3952-3956, 2005.

Appendix A. Summary of pile driving levels

This appendix provides summary tables of mean and maximum measured sound levels from marine pile driving at the Mukilteo test site. Note that sound exposure levels (SEL's) given in the tables are for *single* pile driving impulses. The total sound exposure may be computed from the mean SEL values given in the tables according to the following formula:

$$L_E^{(total)} = L_E^{(mean)} + 10 \log_{10} N$$

where $L_E^{(mean)}$ is the mean sound exposure from the table and N is the total number of pile driving strikes.

Pile: R1
Type: Steel
Mitigation: Foam TNAP
Strikes: 157

Range (m)	Mean					Maximum				
	Peak-to-Peak (dB//μPa)	Peak (dB//μPa)	90% rms (dB//μPa)	SEL (dB//μPa ² s)	90%rms length (msec)	Peak-to-Peak (dB//μPa)	Peak (dB//μPa)	90% rms (dB//μPa)	SEL (dB//μPa ² s)	
10	193.6	188.6	177.9	166.0	58.4	195.6	191.5	179.7	167.1	
50	186.8	181.6	170.7	158.6	55.6	189.7	184.9	171.7	159.6	
100	184.8	179.8	168.8	156.7	55.6	187.8	183.6	171.4	158.8	
1100	164.3	159.0	147.2	137.2	93.5	165.5	160.7	149.4	138.9	

Pile: R2
Type: Steel
Mitigation: No mitigation
Strikes: 19

Range (m)	Mean					Maximum				
	Peak-to-Peak (dB//μPa)	Peak (dB//μPa)	90% rms (dB//μPa)	SEL (dB//μPa ² s)	90%rms length (msec)	Peak-to-Peak (dB//μPa)	Peak (dB//μPa)	90% rms (dB//μPa)	SEL (dB//μPa ² s)	
10	207.6	202.6	192.4	178.1	34.6	211.2	206.2	196.3	180.1	
50	197.8	193.4	182.1	168.7	41.2	200.7	197.0	184.3	170.3	
100	188.9	184.2	172.8	160.6	54.2	191.2	187.8	173.9	161.4	
1100	169.3	164.0	153.8	142.9	73.5	172.1	166.3	156.0	144.7	

Pile: R2
Type: Steel
Mitigation: Bubble curtain
Strikes: 223

Range (m)	Mean					Maximum				
	Peak-to-Peak (dB//μPa)	Peak (dB//μPa)	90% rms (dB//μPa)	SEL (dB//μPa ² s)	90%rms length (msec)	Peak-to-Peak (dB//μPa)	Peak (dB//μPa)	90% rms (dB//μPa)	SEL (dB//μPa ² s)	
10	188.5	183.4	170.2	158.4	60.3	192.6	187.3	173.5	160.6	
50	188.2	183.3	171.9	159.0	46.7	190.5	185.0	173.1	160.0	
100	184.7	179.6	169.5	156.9	48.7	186.7	182.1	171.7	158.6	
1100	165.6	160.2	147.9	137.9	108.2	167.1	161.9	149.7	139.3	

Pile: R3
Type: Steel
Mitigation: Foam TNAP
Strikes: 88

Range (m)	Mean					Maximum				
	Peak-to-Peak (dB//μPa)	Peak (dB//μPa)	90% rms (dB//μPa)	SEL (dB//μPa ² s)	90%rms length (msec)	Peak-to-Peak (dB//μPa)	Peak (dB//μPa)	90% rms (dB//μPa)	SEL (dB//μPa ² s)	
10	188.9	183.5	171.8	161.6	86.8	192.6	188.2	173.9	163.0	
50	187.5	182.6	172.6	160.3	53.7	189.8	185.4	174.8	162.0	
100	185.1	179.5	168.6	156.9	60.4	185.8	180.2	170.2	158.0	
1100	164.2	158.9	148.5	138.4	88.0	166.6	160.9	151.7	140.7	

Pile: R4
Type: Steel
Mitigation: Double-walled TNAP
Strikes: 68

Range (m)	Mean					Maximum				
	Peak-to-Peak (dB//μPa)	Peak (dB//μPa)	90% rms (dB//μPa)	SEL (dB//μPa ² s)	90%rms length (msec)	Peak-to-Peak (dB//μPa)	Peak (dB//μPa)	90% rms (dB//μPa)	SEL (dB//μPa ² s)	
10	203.2	198.0	188.5	174.2	33.5	206.5	202.6	191.0	176.3	
50	198.5	193.7	181.3	167.8	40.4	200.1	195.2	182.6	169.0	
100	192.3	187.4	174.3	161.8	51.1	194.9	189.6	177.3	164.2	
1100	170.0	164.4	153.2	142.0	68.2	171.8	166.8	155.1	143.4	

Pile: T2
Type: Steel
Mitigation: Bubble curtain
Strikes: 81

Range (m)	Mean					Maximum				
	Peak-to-Peak (dB//μPa)	Peak (dB//μPa)	90% rms (dB//μPa)	SEL (dB//μPa ² s)	90%rms length (msec)	Peak-to-Peak (dB//μPa)	Peak (dB//μPa)	90% rms (dB//μPa)	SEL (dB//μPa ² s)	
10	189.8	184.6	171.6	160.4	69.1	192.9	188.2	174.0	161.9	
50	185.1	179.8	168.8	157.2	62.4	188.4	183.1	171.7	159.5	
100	184.2	179.2	168.9	156.2	49.7	187.2	183.5	173.0	159.3	
1100	161.9	156.4	144.5	135.7	152.5	164.4	158.6	146.8	138.9	

Pile: T2
Type: Steel
Mitigation: None
Strikes: 33

Range (m)	Mean					Maximum				
	Peak-to-Peak (dB//μPa)	Peak (dB//μPa)	90% rms (dB//μPa)	SEL (dB//μPa ² s)	90%rms length (msec)	Peak-to-Peak (dB//μPa)	Peak (dB//μPa)	90% rms (dB//μPa)	SEL (dB//μPa ² s)	
10 ^{a)}	—	207.0	201.0	—	—	214.0	—	—	—	
50	201.7	196.5	185.3	171.5	37.5	204.9	199.0	188.2	173.9	
100	193.7	188.5	177.4	163.8	39.4	196.6	190.7	180.8	165.8	
1100	170.4	165.1	152.7	142.7	113.4	173.4	168.3	155.4	144.3	

a) Unmitigated waveform data for pile T2 were unavailable for analysis at the time of writing. However, values for the peak and rms levels for this pile were provided by Jim Laughlin, WSDOT.

Underwater Acoustic Measurements: Test Pile Project 2006

Pile: T3
Type: Concrete
Mitigation: None
Strikes: 572

Range (m)	<i>Mean</i>					<i>Maximum</i>			
	Peak-to-Peak (dB//μPa)	Peak (dB//μPa)	90% rms (dB//μPa)	SEL (dB//μPa ² s)	90%rms length (msec)	Peak-to-Peak (dB//μPa)	Peak (dB//μPa)	90% rms (dB//μPa)	SEL (dB//μPa ² s)
50	189.7	184.0	174.6	161.2	41.6	191.8	186.2	177.1	163.3
200	172.4	167.8	157.1	145.6	66.8	174.3	170.1	159.7	147.9

Pile: T4
Type: Concrete
Mitigation: None
Strikes: 1626

Range (m)	<i>Mean</i>					<i>Maximum</i>			
	Peak-to-Peak (dB//μPa)	Peak (dB//μPa)	90% rms (dB//μPa)	SEL (dB//μPa ² s)	90%rms length (msec)	Peak-to-Peak (dB//μPa)	Peak (dB//μPa)	90% rms (dB//μPa)	SEL (dB//μPa ² s)
50	192.7	187.7	176.0	163.1	47.1	195.1	190.7	179.0	164.4
200	181.7	176.5	164.8	153.3	63.6	183.8	179.2	166.9	154.4